Template-Directed Molecular Assembly on Silicon Carbide Nanomesh: Comparison Between CuPc and Pentacene

Chen Shi,[†,‡] Chen Wei,[†,‡] Huang Han,[†] Gao Xingyu,[†,*] Qi Dongchen,[†] Wang Yuzhan,[†] and Andrew T. S. Wee[†,*]

[†]Department of Physics and [‡]Department of Chemistry, National University of Singapore, 3 Science Drive 3, 117543, Singapore

ABSTRACT The template-directed assembly of two planar molecules (copper phthalocyanine (CuPc) and pentacene) on SiC nanomesh has been studied by scanning tunneling microscopy and photoelectron spectroscopy, respectively. Both molecules are trapped as single molecules in the cells of SiC nanomesh at low coverage. At high coverage, CuPc forms a highly ordered single-molecular array with identical symmetry and periodicity as the substrate, whereas pentacene forms a quasi-amorphous layer due to the random mixture of three different adsorption configurations. This difference in adsorption behavior is attributed to differences in molecular geometries. The measured changes of work functions reveal weak charge transfer between the molecules and substrate. Both molecules are preferentially adsorbed on the SiC nanomesh rather than on graphene. The CuPc single-molecular array possesses good long-range order, large area coverage, and a molecular density of over 3.0 $\times$ 10^{13} molecules/cm^2.

KEYWORDS: SiC · nanomesh · copper phthalocyanine · pentacene · STM · template

Reducing the size of devices is the driving force of modern nanotechnology.[1] As the smallest building block for nanodevices, many molecules have been extensively investigated and built to work as single-molecule-based devices.[2,3] However, one major challenge is how to condense molecules onto a surface without aggregation. One viable method is to employ supramolecular architectures that can be self-assembled at vacuum/solid or liquid/solid interfaces using surface templates to isolate guest molecules *via* host−guest interactions.[4−18] Among all demonstrated templates, the naturally formed corrugated surfaces[11−13] are the most promising due to their stability. Nevertheless, the dimensions of the corrugations in these surfaces are usually larger than the molecule; hence the resulting arrays are composed of molecular clusters instead of isolated single molecules. Thus, corrugated surfaces with shorter periodicity are needed for the construction of single molecular arrays for applications such as biosensors and data storage. One good example is the BN nanomesh with 2 nm hole and 3.2 nm lattice constant. This template has been demonstrated to trap single molecules or atoms inside its "holes".[19] Another corrugated surface, the $6\sqrt{3} \times 6\sqrt{3}$ R30° reconstructed 6H-SiC(0001) surface (henceforth referred to as "SiC nanomesh"[20,21]), with a periodicity of about 1.95 nm is another potential candidate for the formation of molecular arrays. However, the deposition of C_{60} on SiC nanomesh resulted in a close-packed wetting layer due to stronger intermolecular interactions relative to the molecule−nanotemplate interaction.[22]

In this work, the adsorption of two planar molecules, CuPc and pentacene, is studied on the SiC nanomesh surface prepared by thermal annealing of a 6H-SiC(0001) sample. STM and PES are used to investigate the adsorption geometries as well as the adsorption interactions. STM measurement reveals that both molecules are selectively adsorbed in the nanomesh cells with three different orientations. However, at high coverage, the assembly of these two molecules is quite different. CuPc forms an ordered single-molecular array which uniformly covers the whole surface. This array has the periodicity and rotational symmetry identical to those of the substrate, indicating that the molecules are directly confined by the SiC nanomesh. Moreover, the distance between adjacent molecules is larger than the dimension of the molecule, implying that the individual CuPc molecules are noninteracting and this array is a perfectly isolated molecular array. On the other hand, the molecules of pentacene, which has

*Address correspondence to phygaoxy@nus.edu.sg, phyweets@nus.edu.sg.

Received for review October 23, 2009 and accepted December 30, 2009.

Published online January 5, 2010. 10.1021/nn901476m

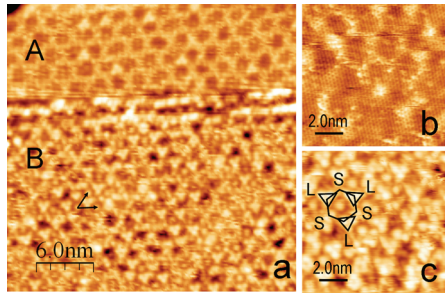

Figure 1. STM images of SiC nanomesh/graphene mixed phase surface: (a) large area scan (30 × 30 nm^2, V_T = 2.1 V, I_T = 70 pA); (b) enlarged image of terrace A (10 × 10 nm^2, V_T = 0.5 V, I_T = 70 pA), (c) enlarged image of terrace B (10 × 10 nm^2, V_T = 2.1 V, I_T = 70 pA).

multiple adsorption configurations at high coverage, are mixed randomly to form a quasi-amorphous layer on the SiC nanomesh.

RESULTS AND DISCUSSION

The clean SiC nanomesh surface is shown in Figure 1. Unlike the sample for XPS measurements, this sample is slightly over-annealed to produce a nanomesh/graphene mixed phase surface. The terrace A in Figure 1a is covered by epitaxial graphene (EG), as shown in corresponding zoom-in Figure 1b. The terrace B, which comprises SiC nanomesh with 1.95 nm honeycomb-like cells, is enlarged in Figure 1c. From this image, several distinct features of SiC nanomesh can be distinguished. First of all, three out of six corners of the hexagonal cells appear as bright triangular clusters (triangles at hexagon corners).[23] Meanwhile, the other three corners are featureless. In this work, the corners with bright triangles are labeled "L" while the featureless vertices are labeled "S". The L and S vertices are not precisely located at the hexagon corners (Figure 1c). This is due to the surface irregularity of the SiC nanomesh.[22] Another prominent feature is the bumps in the middle of the cells. This feature was observed in the work presented in previous papers,[20,23,24] but its origin is not understood.

After a nominal dosage about 0.1 monolayer (ML), single CuPc molecules appear as four-leaved clovers as shown in Figure 2. The dosage is estimated according to the size of the CuPc molecules (1.4 × 1.4 nm^2) in its closed packed form on highly oriented pyrolytic graphite (HOPG).[25] The simultaneously resolved triangular clusters of the SiC nanomesh are used as a reference grid to determine the adsorption configurations of CuPc. In Figure 2a, CuPc molecules lie directly above the nanomesh pores with their four lobes extended to the rims of the nanomesh cells. This is a clear indication that the growth of CuPc is mediated by the SiC nanomesh. Furthermore, adsorbed CuPc molecules follow the orientation of the substrate. To clarify the orientations of CuPc, a vector pointing from the center copper atom outward in between the two lobes is used to indicate the in-plane orientation of CuPc (black arrows in

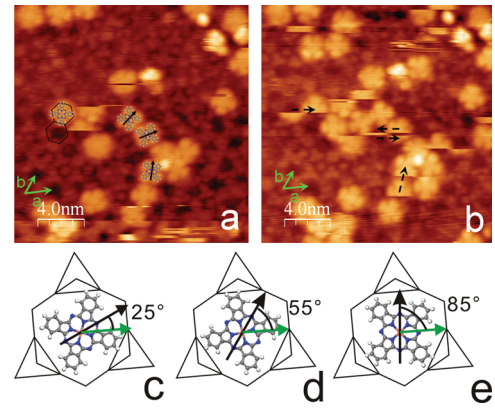

Figure 2. CuPc molecules on SiC nanomesh: (a) adsorbed CuPc molecules; (b) hopping of single molecules under tip perturbation (conditions for panels a and b: 20 × 20 nm^2, V_T = 3.4 V, I_T = 40 pA); (c−e) schematic models of the three CuPc orientations on SiC nanomesh cells. Black arrows indicate the orientations of CuPc; green arrows indicate the *a* axis of SiC nanomesh.

Figure 2a). Three orientations (25 ± 3°, 55 ± 3°, and 85 ± 3°: the error-bars are estimated by statistical average of molecular orientations in several STM images) relative to the substrate *a* axis are shown in Figure 2a. To elucidate these orientations, schematic pictures of CuPc with three different orientations as well as the SiC nanomesh cells are shown in Figure 2c−e. The three orientations are actually degenerate due to the 3-fold symmetry of the substrate. However, after adsorption of multiple CuPc molecules, the substrate-induced degeneracy is removed and the three orientations of CuPc become distinguishable. Owing to the 4-fold symmetry of CuPc, any orientation angle larger than 90° can be automatically reflected back to the first quadrant. As the result, the angles determined by 3-fold substrate symmetry (θ, θ + 120°, and θ + 240°) are reduced into θ, θ + 30°, and θ + 60°. This deduction successfully explains the 30° angular difference of the three orientations.

In Figure 2b, some CuPc molecules appear as complementary fragments at several locations; this is possibly due to molecular hopping by either thermal activation or tip perturbation. As the acquisition time of Figure 2b is 471 at 0.75 s per line, the sudden appearance/disappearance of CuPc molecules indicates a much shorter hopping time than 0.75 s. In addition, the hopping frequency or dwell time of CuPc molecules can be estimated experimentally. About 17 hopping events are counted over 34 molecules during the acquisition of Figure 2b. The hopping for a single molecule thus happens roughly once per 1 × 10^3 seconds at low dosage. No rotation of the static CuPc molecules in sequential STM images is observed, but molecules may change their orientations during hopping. In a few cases, CuPc molecules may hop back to their original sites (back and forth dashed arrows in Figure 2b), or new molecules may hop to previously occupied sites (not shown here). These molecules adopt the same orientation of the previous molecules at these sites, imply-

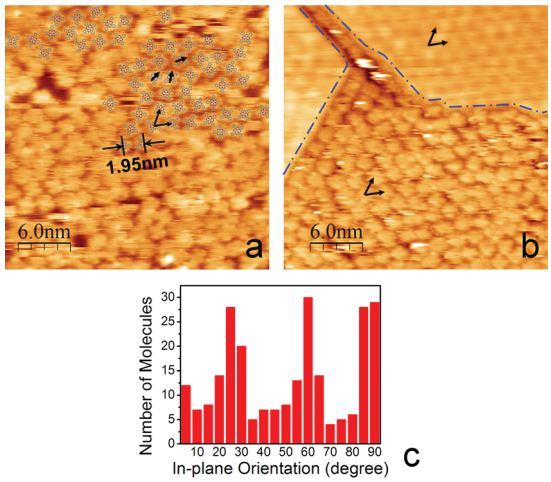

Figure 3. The CuPc single-molecular array on the SiC nanomesh surface: (a) 30 × 30 nm^2 STM image of the CuPc molecular array ($V_T = -1.9$ V, $I_T = 40$ pA); (b) 30 × 30 nm^2 STM image of the CuPc molecular array on a nanomesh terrace ($V_T = -2.2$ V, $I_T = 40$ pA); (c) statistics of the in-plane orientations of CuPc molecules.

ing that in one cell, only one out of three symmetric in-plane orientations is energetically favorable. The hopping happens frequently at low dosage, suggesting that the energy barrier for hopping is small when the neighboring pore site is unoccupied.

At 0.4 ML coverage, CuPc molecules are evenly distributed on the SiC nanomesh surface forming an ordered single-molecular array, as shown in Figure 3a. This array possesses a 1.95 nm periodicity and 3-fold symmetry of the substrate. The periodicity of the CuPc array is not only larger than the CuPc size in its closed packed form (about 1.4 nm),[25,26] but also larger than the calculated maximum size of the CuPc molecule (1.68 nm in diagonal length).[27] The large separation (2.7 Å or larger) and arbitrary orientations of adjacent molecules suggest negligible intermolecular interactions. As most molecular orientations can be distinguished in Figure 3a, a statistical analysis is performed to study the distribution of these orientations. Three peaks at 25°, 60°, and 90° are observed, indicating the preferred in-plane orientations of CuPc molecules. These angles are similar to the orientation of CuPc molecules at low coverage. Thus, both spatial locations and orientations of CuPc are confined by the substrate to form an ordered single molecular array.

In Figure 3b, the CuPc array is observed to cover the lower terrace uniformly, while the upper two terraces covered by single-layer graphene (SLG) are totally empty, suggesting the preferential adsorption of CuPc on SiC nanomesh instead of on graphene. This is not surprising since the graphene/graphite surface is known to be unreactive. The formation of this molecular array is not limited to selected nanomesh terraces; on the contrary, this array is observed on all the SiC nanomesh terraces forming a wafer-scale single molecular

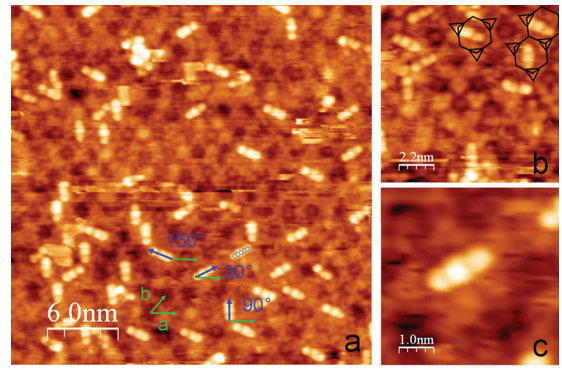

Figure 4. Pentacene molecules on SiC nanomesh: (a) 30 × 30 nm^2 STM image of pentacene on SiC nanomesh ($V_T = 1.7$ V, $I_T = 40$ pA). Blue arrows indicates the orientation of pentacene molecules and green arrows indicates the *a* axis of the substrate. (b) The enlarged image shows the location of pentacene on the SiC nanomesh. The hexagons indicate the SiC nanomesh cells, and the triangles indicate the L vertices. (c) The enlarged image of a single pentacene molecule.

array. The molecular density of this array is estimated to be about 3.0 × 10^{13} molecules/cm^2.

We next study another molecule with simple geometry, pentacene, to probe the molecular adsorption sites on this nanomesh surface. Figure 4a shows the STM image of pentacene deposited on SiC nanomesh at low coverage (~0.2 ML). The rodlike feature represents a single pentacene molecule lying flat. Because of the different molecule−substrate couplings, the submolecular features of pentacene vary from one substrate to another.[28−31] In Figure 4c, pentacene appears as three bright protrusions.

As with the CuPc molecules, pentacene adsorbs within the cells and points to the corners of these cells. The magnified image (Figure 4b) shows that the pentacene molecules deviate slightly from the center of the cells with one phenyl end closer to the L vertex. The orientations of adsorbed pentacene molecules are coincident with the direction from the cell center to L vertex and about 30°, 90°, and 150° degrees to the substrate *a* axis. Unlike CuPc, the fragmented pentacene image is not observed in Figure 4. Thus the hopping time of pentacene cannot be monitored by STM scanning. Instead, the hopping of pentacene is counted by the appearance/disappearance of molecules in sequential images. The events are rare (less than 1 hopping event over 100 molecules in one scan), indicating that the trapping of pentacene is much stronger than CuPc. The dwell time of pentacene is >4 × 10^4 seconds based on the number of hopping events observed.

From the STM studies, both molecules are trapped in the cell with substrate-determined orientations. These observations imply that these molecules are trapped not only by the cell centers but also by the vertices of the cells. In the case of pentacene, the L vertex appears to interact more strongly with pentacene than the S vertex. In the case of CuPc, the molecular lobes lie in-between the L and S vertices, possibly due to the

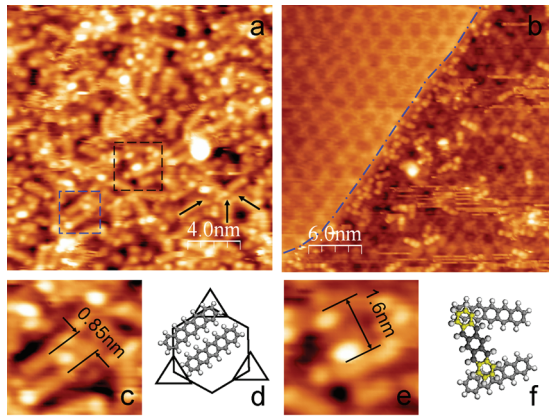

Figure 5. Quasi-amorphous pentacene layer on SiC nanomesh: (a) 0.8 ML pentacene on SiC nanomesh (20 × 20 nm², $V_T = -1.9$ V, $I_T = 40$ pA); (b) pentacene at the domain boundary (30 × 30 nm², $V_T = 1.9$ V, $I_T = 40$ pA); (c) enlarged image shows the parallel configuration from the blue square in panel a; (d) schematic of parallel configuration in honeycomb cell. This two-in-one configuration is geometrically possible; (e) enlarged image shows the bridge configuration from the black square in panel a; (f) schematic of bridge configuration. The two ends of upper pentacene are colored in yellow to indicate the bright dots in panel e.

competing interactions between the molecule and the L and S vertices. Although the atomic structure of these nanomesh features are not fully understood, these cells and vertices effectively trap CuPc and pentacene molecules to form molecular arrays.

When the dosage of pentacene increases to 0.8 ML, molecules reside on the SiC nanomesh with less order. However, three types of adsorption configurations can be distinguished on this surface. First of all, small numbers of molecules possess the 3-fold symmetric configuration and they are highlighted by the black arrows in Figure 5a. The second configuration is where the molecules pack in parallel (Figure 5c). In this configuration, the intermolecular distance is about 0.85 nm, much less than the periodicity of SiC nanomesh (1.95 nm), implying that two molecules reside in one SiC nanomesh cell (Figure 5d). The last distinguishable configuration is the bridge configuration, whereby the molecules appear as two bright dots separated by a gap (Figure 5e). A similar appearance of pentacene described as a "two-lobe structure" has been reported at the second pentacene layer on Ag(111).[32] Although the authors did not discuss the origin of this "two-lobe structure", we infer from their STM images that this structure is due to a pentacene molecule crossing two underlying ones. Therefore, the appearance here could be regarded as one molecule bridging two underlying molecules (Figure 5f). A similar pentacene image with three bright dots and two dark gaps has been observed by Kasaya *et al.*[33] on silicon (100) 2 × 1, and the authors explained the image by a model where pentacene molecules bridge three dimer rows. The mixture of these configurations at high coverage could be explained by two reasons. The first is the small size of pentacene (1.66 × 0.74 nm)[34] relative to the nanomesh cell. The space between two pentacene molecules in neighboring cells is large enough to accommodate additional molecules in metastable configurations, that is, the parallel and bridge configurations. Therefore, the small size of pentacene allows disorder in the molecular array at higher coverage. The second reason is attributed to the limited diffusivity of pentacene molecules on the SiC nanomesh. In Figure 5b, a domain boundary between graphene and SiC nanomesh is indicated by the dashed line. It can be clearly observed that no pentacene molecules adsorb on graphene, and that the population of pentacene increases on the SiC nanomesh close to this boundary. The increase in population is due to the unidirectional diffusion of pentacene from graphene to the nanomesh surface. The same diffusion trend was suggested in CuPc deposition, but the diffusivity of CuPc on SiC nanomesh is large enough to distribute the excess molecules away from the boundary (cf. Figure 3b). Pentacene therefore forms a random array at high coverage due to multiple adsorption configurations and low diffusivity.

We have investigated the template effect of the SiC nanomesh by two molecules, CuPc and pentacene. The adsorption geometries of both molecules are constrained by the nanomesh substrate. CuPc is demonstrated to form a highly ordered single molecular array, whereas pentacene forms a random array comprising several intermixed configurations. Next, photoelectron studies of both molecule−substrate systems will help to clarify the origin of this interaction.

While no chemical reactions could be identified from XPS (see Supporting Information), small work function shifts for CuPc (−0.15 ± 0.05 eV) and pentacene (−0.25 ± 0.05 eV) are observed (Figure 6). This suggests a vacuum level shift relative to the Fermi level due to the formation of interface dipoles, which originate from electron transfer from CuPc or pentacene (electron donor)[35−37] to the SiC nanomesh. As previously reported,[22] the weak charge transfer between C_{60} and SiC nanomesh, which induces a +0.15 ± 0.05 eV vacuum level shift, is responsible for altering the fullerene growth from island mode to layer-by-layer mode within the first two layers. Therefore, the interaction which traps CuPc and pentacene inside the cells of SiC nanomesh is attributed to the weak interface dipoles. The relative dipole strengths can explain the different hopping rate of the two molecules. Due to the weaker dipole force, CuPc is more uniformly distributed on the SiC nanomesh surface. Meanwhile, the stronger dipole force hinders the diffusion of pentacene on the nanomesh surface and results in an accumulation of molecules at the graphene−nanomesh phase boundary.

The dipole force is responsible for trapping both molecules on the SiC nanomesh surface, but it may not be enough to explain the differences in molecular assembly. In the experiments, the size and geometry of

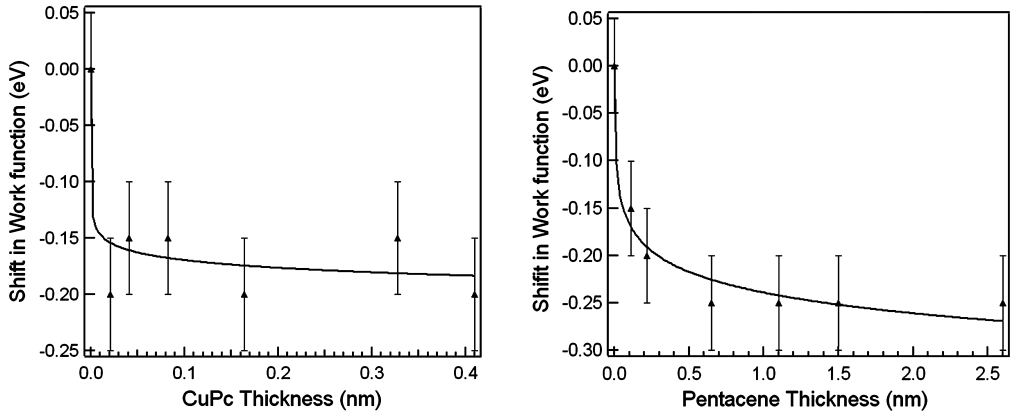

Figure 6. Work function change after adsorption of (a) CuPc, (b) pentacene.

the molecules also influences the molecular assembly. The formation of an ordered array for CuPc is facilitated by its compatible size to the nanomesh cell. The square-shaped Van-der-Waals envelope of CuPc (1.68 nm) is slightly smaller than the periodicity of SiC nanomesh (1.95 nm) and forms a one-molecule-in-one-cell configuration. The CuPc size is large enough to exclude a two-in-one configuration. However, the pentacene molecule with smaller Van-der-Waals envelope (1.66 nm $\times$ 0.74 nm) allows a two-in-one configuration in the nanomesh. Thus, the size of molecules plays a crucial role in the formation of ordered single molecular arrays.

Although both molecules have three in-plane orientations, the angular difference of orientations is 30° for CuPc while it is 60° for pentacene. This difference is due to the 4-fold and 2-fold symmetry of CuPc and pentacene, respectively. If a 3-fold or 6-fold symmetric molecule is used, the adsorbed molecules will only have one in-plane orientation and form a higher ordered molecular array.

CONCLUSION

The template effect of SiC nanomesh was observed in CuPc and pentacene deposition. The adsorption configurations of both molecules are influenced by the substrate, revealing the template effect of the nanomesh surface. In particular, CuPc forms a highly ordered single molecular array covering the nanomesh uniformly. This array maintains the periodicity and symmetry of the substrate. In contrast, pentacene forms a quasi-amorphous overlayer comprising a random mixture of several different configurations. From photoelectron measurements, no chemical shift was identified except for small work function shifts for CuPc (-0.15 ± 0.05 eV) and pentacene (-0.25 ± 0.05 eV). These shifts are explained by the formation of interface dipoles induced by charge transfer. The formation of such molecular arrays with ultra high density and large area on the SiC nanomesh surface has potential applications in high-density data storage and chemical sensors.

METHODS

The SiC nanomesh on a 6H-SiC(0001) sample (CREE Research, Inc.) was prepared in the multichamber endstation of the Surface, Interface, and Nanostructure Science (SINS) beamline, Singapore Synchrotron Light Source.[38] The SiC sample was directly heated at 700 °C for overnight degassing and followed by annealing with additional Si flux at 800 °C to remove native oxide on the surface. Then the sample was annealed to 1150 °C to form the SiC nanomesh surface. The sample preparation is described in detail elsewhere.[20] The synchrotron-based photoelectron experiments were performed *in situ* in the same system. The synchrotron light is p-polarized with photon energy resolution $E/\Delta E$ set at about 1000. A hemispherical electron energy analyzer (EA 125, Omicrometer Nano-Technology GmbH) is used to analyze the photoelectron. The photon energy is set at 350 eV for C 1s and Si 2p measurements, and 60 eV for work function measurement. Photon incident angle is set to 50° to surface normal, and photoemitted electrons are collected at 90°. The STM experiments for CuPc and pentacene deposition were conducted in a low temperature STM system.[39] Another nanomesh sample was carefully degassed to remove contaminations after the ex-situ transfer. The clean nanomesh surfaces were observed by STM measurement and are consistent with previous reports.[20,23] Organic molecules were evaporated by using a low-temperature Knudsen cell (MBE-Komponenten, Germany) onto SiC nanomesh substrates at room temperature. The deposition temperatures for CuPc (Sigma-Aldrich, sublimation grade) and pentacene (Sigma-Aldrich, 99.9%, sublimed) are 350 and 190 °C, respectively. During deposition, the chamber pressure was always maintained below 1.0×10^{-9} Torr. The deposition rate is calibrated either by using the attenuation of the Au 4f photoelectron peak after deposition of molecules on a reference Au(100) sample in XPS measurement or by measuring the molecular coverage in STM images. To resolve the low kinetic energy electrons cutoff, a negative 5 V sample bias was applied. The vacuum level (E_{vac}) of SiC nanomesh upon the deposition of CuPc or pentacene was measured by linear extrapolation of the low-kinetic energy onset (secondary electron cutoff) of PES spectra.[40]

Acknowledgment. Authors acknowledge the support from the Singapore A*STAR Grant R-398-000-036-305 and ARF Grants R-144-000-196-112 and R-143-000-392-133.

Supporting Information Available: Photoelectron spectra of CuPc deposition (C 1s, Si 2p, and Cu 2p) and pentacene deposition (C 1s and Si 2p) on SiC nanomesh. This material is available free of charge *via* the Internet at http://pubs.acs.org.

REFERENCES AND NOTES

1. Feynman, R. There's Plenty of Room at Bottom. *Eng. Sci.* **1960**, *23*, 22–36.

2. Joachim, C.; Gimzewski, J. K.; Aviram, A. Electronics Using Hybrid-Molecular and Mono-Molecular Devices. *Nature* **2000**, *408*, 541–548.
3. Kay, E. R.; Leigh, D. A.; Zerbetto, F. Synthetic Molecular Motors and Mechanical Machines. *Angew. Chem., Int. Ed.* **2007**, *46*, 72–191.
4. Spillmann, H.; Kiebele, A.; Stöhr, M.; Jung, T. A.; Bonifazi, D.; Cheng, F.; Diederich, F. A Two-Dimensional Porphyrin-Based Porous Network Featuring Communicating Cavities for the Templated Complexation of Fullerenes. *Adv. Mater.* **2006**, *18*, 275–279.
5. Stepanow, S.; Lingenfelder, M.; Dmitriev, A.; Spillmann, H.; Delvigne, E.; Lin, N.; Deng, X. B.; Cai, C. Z.; Barth, J. V.; Kern, K. Steering Molecular Organization and Host-Guest Interactions Using Two-Dimensional Nanoporous Coordination Systems. *Nat. Mater.* **2004**, *3*, 229–233.
6. Chen, W.; Zhang, H. L.; Huang, H.; Chen, L.; Wee, A. T. S. Self-Assembled Organic Donor/Acceptor Nanojunction Arrays. *Appl. Phys. Lett.* **2008**, *92*, 193301.
7. Zhang, H. L.; Chen, W.; Huang, H.; Chen, L.; Wee, A. T. S. Preferential Trapping of C-60 in Nanomesh Voids. *J. Am. Chem. Soc.* **2008**, *130*, 2720–2721.
8. Stepanow, S.; Lin, N.; Barth, J. V.; Kern, K. Non-Covalent Binding of Fullerenes and Biomolecules at Surface-Supported Metallosupramolecular Receptors. *Chem. Commun.* **2006**, 2153–2155.
9. Pan, G. B.; Liu, J. M.; Zhang, H. M.; Wan, L. J.; Zheng, Q. Y.; Bai, C. L. Configurations of a Calix[8]arene and a C-60/Calix[8]arene Complex on a Au(111) Surface. *Angew. Chem., Int. Ed.* **2003**, *42*, 2747–2751.
10. Staniec, P. A.; Perdigão, L. M. A.; Saywell, A.; Champness, N. R.; Beton, P. H. Hierarchical Organisation on a Two-Dimensional Supramolecular Network. *Chem. Phys. Chem.* **2007**, *8*, 2177–2181.
11. Néel, N.; Kröger, J.; Berndt, R. Highly Periodic Fullerene Nanomesh. *Adv. Mater.* **2006**, *18*, 174–177.
12. Böhringer, M.; Morgenstern, K.; Schneider, W.-D.; Berndt, R.; Mauri, F.; Vita, A. D.; Car, R. Two-Dimensional Self-Assembly of Supramolecular Clusters and Chains. *Phys. Rev. Lett.* **1999**, *83*, 324–327.
13. Corso, M.; Auwärter, W.; Muntwiler, M.; Tamai, A.; Greber, T.; Osterwalder, J. Boron Nitride Nanomesh. *Science* **2004**, *303*, 217–220.
14. Li, S. S.; Northrop, B. H.; Yuan, Q. H.; Wan, L. J.; Stang, P. J. Surface Confined Metallosupramolecular Architectures: Formation and Scanning Tunneling Microscopy Characterization. *Acc. Chem. Res.* **2009**, *42*, 249–259.
15. Lei, S. B.; Tahara, K.; Feng, X. L.; Furukawa, S. H.; De Schryver, F. C.; Mullen, K.; Tobe, Y.; De Feyter, S. Molecular Clusters in Two-Dimensional Surface-Confined Nanoporous Molecular Networks: Structure, Rigidity and Dynamics. *J. Am. Chem. Soc.* **2008**, *130*, 7119–7129.
16. Ma, X. J.; Yang, Y. L.; Deng, K.; Zeng, Q. D.; Zhao, K. Q.; Wang, C.; Bai, C. L. Molecular Miscibility Characteristic of Self-Assembled 2D Molecular Architectures. *J. Mater. Chem.* **2008**, *18*, 2074–2081.
17. Yoshimoto, S.; Honda, Y.; Ito, O.; Itaya, K. Supramolecular Pattern of Fullerene on 2D Bimolecular "Chessboard" Consisting of Bottom-up Assembly of Porphyrin and Phthalocyanine Molecules. *J. Am. Chem. Soc.* **2008**, *130*, 1085–1092.
18. Kudernac, T.; Lei, S. B.; Elemans, J. A. A. W.; De Feyter, S. ; Two-Dimensional Supramolecular Self-Assembly: Nanoporous Network on Surfaces. *Chem. Soc. Rev.* **2009**, *38*, 402–421.
19. Dil, H.; Lobo-Checa, J.; Laskowski, R.; Blaha, P.; Berner, S.; Osterwalder, J.; Greber, T. Surface Trapping of Atoms and Molecules with Dipole Rings. *Science* **2008**, *319*, 1824–1826.
20. Chen, W.; Xu, H.; Liu, L.; Gao, X. Y.; Qi, D. C.; Peng, G. W.; Tan, S. C.; Feng, Y. P.; Loh, K. P.; Wee, A. T. S. Atomic Structure of the 6H-SiC(0001) Nanomesh. *Surf. Sci.* **2005**, *596*, 176–186.
21. Chen, W.; Wee, A. T. S. Self-Assembly on Silicon Carbide Nanomesh Templates. *J. Phys. D* **2007**, *40*, 6287–6299.
22. Chen, W.; Chen, S.; Zhang, H. L.; Xu, H.; Qi, D. C.; Gao, X. Y.; Loh, K. P.; Wee, A. T. S. Probing the Interaction at the C-60-SiC Nanomesh Interface. *Surf. Sci.* **2007**, *601*, 2994–3002.
23. Riedl, C.; Starke, U.; Bernhardt, J.; Franke, M.; Heinz, K. Structural Properties of the Graphene-SiC(0001) Interface as a Key for the Preparation of Homogeneous Large-Terrace Graphene Surfaces. *Phys. Rev. B* **2007**, *76*, 245406.
24. Owman, F.; Mårtensson, P. High-Resolution Core-Level Study of 6H-SiC(0001). *Surf. Sci.* **1996**, *369*, 126–136.
25. Wang, S. D.; Dong, X.; Lee, C. S.; Lee, S. T. Orderly Growth of Copper Phthalocyanine on Highly Oriented Pyrolytic Graphite (HOPG) at High Substrate Temperatures. *J. Phys. Chem. B* **2004**, *108*, 1529–1532.
26. Ludwig, C.; Strohmaier, R.; Petersen, J.; Gompf, B.; Eisenmenger, W. Epitaxy and Scanning-Tunneling-Microscopy Image-Contrast of Copper Phthalocyanine on Graphite and MoS_2. *J. Vac. Sci. Technol. B* **1994**, *12*, 1963–1966.
27. Manandhar, K.; Ellis, T.; Park, K. T.; Cai, T.; Song, Z.; Hrbek, J. A Scanning Tunneling Microscopy Study on the Effect of Post-Deposition Annealing of Copper Phthalocyanine Thin Films. *Surf. Sci.* **2007**, *601*, 3623–3631.
28. Chen, W.; Huang, H.; Wee, A. T. S. Molecular Orientation Transition of Organic Thin Films on Graphite: The Effect of Intermolecular Electrostatic and Interfacial Dispersion Forces. *Chem. Commun.* **2008**, 4276–4278.
29. Suzuki, T.; Sorescu, D. C.; Yates, J. T., Jr. The Chemisorption of Pentacene on Si(001)-2 × 1. *Surf. Sci.* **2006**, *600*, 5092–5103.
30. Choudhary, D.; Clancy, P.; Bowler, D. R. Adsorption of Pentacene on a Silicon Surface. *Surf. Sci.* **2005**, *578*, 20–26.
31. Repp, J.; Meyer, G.; Stojković, S. M.; Gourdon, A.; Joachim, C. Molecules on Insulating Films: Scanning-Tunneling Microscopy Imaging of Individual Molecular Orbitals. *Phys. Rev. Lett.* **2005**, *94*, 026803.
32. Dougherty, D. B.; Jin, W.; Cullen, W. G.; Reutt-Robey, J. E.; Robey, S. W. Variable Temperature Scanning Tunneling Microscopy of Pentacene Monolayer and Bilayer Phases on Ag(111). *J. Phys. Chem. C* **2008**, *112*, 20334–20339.
33. Kasaya, M.; Tabata, H.; Kawai, T. Scanning Tunneling Microscopy and Molecular Orbital Calculation of Pentacene Molecules Adsorbed on the Si(100)2 × 1 Surface. *Surf. Sci.* **1998**, *400*, 367–374.
34. Casalis, L.; Danisman, M. F.; Nickel, B.; Bracco, G.; Toccoli, T.; Iannotta, S.; Scoles, G. Hyperthermal Molecular Beam Deposition of Highly Ordered Organic Thin Films. *Phys. Rev. Lett.* **2003**, *90*, 206101.
35. Qi, D. C.; Gao, X. Y.; Wang, L.; Chen, S.; Loh, K. P.; Wee, A. T. S. Tailoring the Electron Affinity and Electron Emission of Diamond (100) 2 × 1 by Surface Functionalization Using an Organic Semiconductor. *Chem. Mater.* **2008**, *20*, 6871–6879.
36. Hughes, G.; Carty, D.; Cafolla, A. A. Core Level Photoemission Studies of the Interaction of Pentacene with the Si(111) (7 × 7) Surface. *Surf. Sci.* **2005**, *582*, 90–96.
37. Hughes, G.; Carty, D.; McDonald, O.; Cafolla, A. A. Synchrotron Radiation Photoemission Studies of the Pentacene—Ag/Si(111) $\sqrt{3} \times \sqrt{3}$ Interface. *Surf. Sci.* **2005**, *580*, 167–172.
38. Yu, X. J.; Wilhelmi, O; Moser, H. O.; Vidyaraj, S. V.; Gao, X. Y.; Wee, A. T. S.; Nyunt, T.; Qian, H. J.; Zheng, H. W. New Soft X-ray Facility SINS for Surface and Nanoscale Science at SSLS. *J. Electron Spectrosc. Relat. Phenom.* **2005**, *144−147*, 1031–1034.
39. Zhang, H. L.; Chen, W.; Chen, L.; Huang, H.; Wang, X. S.; Yuhara, J.; Wee, A. T. S. C-60 Molecular Chains on α-Sexithiophene Nanostripes. *Small* **2007**, *3*, 2015–2018.
40. Ishii, H.; Sugiyama, K.; Ito, E.; Seki, K. Energy Level Alignment and Interfacial Electronic Structures at Organic/Metal and Organic/Organic Interfaces. *Adv. Mater.* **1999**, *11*, 605–625.